

This discussion paper is/has been under review for the journal Atmospheric Chemistry and Physics (ACP). Please refer to the corresponding final paper in ACP if available.

α -pinene photooxidation under controlled chemical conditions – Part 2: SOA yield and composition in low- and high-NO_x environments

N. C. Eddingsaas¹, C. L. Loza¹, L. D. Yee², M. Chan², K. A. Schilling¹,
P. S. Chhabra^{1,*}, J. H. Seinfeld^{1,2}, and P. O. Wennberg^{2,3}

¹Division of Chemistry and Chemical Engineering, California Institute of Technology, Pasadena, CA, USA

²Division of Engineering and Applied Science, California Institute of Technology, Pasadena, CA, USA

³Division of Geological and Planetary Sciences, California Institute of Technology, Pasadena, CA, USA

*now at: Aerodyne Research Inc, Billerica, MA, USA

Received: 2 March 2012 – Accepted: 19 March 2012 – Published: 4 April 2012

Correspondence to: N. C. Eddingsaas (eddingsa@caltech.edu)

Published by Copernicus Publications on behalf of the European Geosciences Union.

α -pinene photooxidation particle phase composition

N. C. Eddingsaas et al.

Title Page

Abstract

Introduction

Conclusions

References

Tables

Figures

⏪

⏩

◀

▶

Back

Close

Full Screen / Esc

Printer-friendly Version

Interactive Discussion

Abstract

The gas-phase oxidation of α -pinene produces a large amount of secondary organic aerosol (SOA) in the atmosphere. A number of carboxylic acids, organosulfates and nitrooxy organosulfates associated with α -pinene have been found in field samples and some are used as tracers of α -pinene oxidation. α -pinene reacts readily with OH and O_3 in the atmosphere followed by reactions with both HO_2 and NO. Due to the large number of potential reaction pathways, it can be difficult to determine what conditions lead to SOA. To better understand the SOA yield and chemical composition from low- and high- NO_x OH oxidation of α -pinene, studies were conducted in the Caltech atmospheric chamber under controlled chemical conditions. Experiments used low O_3 concentrations to ensure that OH was the main oxidant and low α -pinene concentrations such that the peroxy radical (RO_2) reacted primarily with either HO_2 under low- NO_x conditions or NO under high- NO_x conditions. SOA yield was suppressed under conditions of high-NO. SOA yield under high-NO conditions was greater when ammonium sulfate/sulfuric acid seed particles (highly acidic) were present prior to the onset of growth than when ammonium sulfate seed particles (mildly acidic) were present; this dependence was not observed under low- NO_x conditions. When aerosol seed particles were introduced after OH oxidation, allowing for later generation species to be exposed to fresh inorganic seed particles, a number of low- NO_x products partitioned to the highly acidic aerosol. This indicates that the effect of seed acidity and SOA yield might be under-estimated in traditional experiments where aerosol seed particles are introduced prior to oxidation. We also identify the presence of a number of carboxylic acids that are used as tracer compounds of α -pinene oxidation in the field as well as the formation of organosulfates and nitrooxy organosulfates. A number of the carboxylic acids were observed under all conditions, however, pinic and pinonic acid were only observed under low- NO_x conditions. Evidence is provided for particle-phase sulfate esterification of multi-functional alcohols.

α -pinene photooxidation particle phase composition

N. C. Eddingsaas et al.

Title Page

Abstract

Introduction

Conclusions

References

Tables

Figures



Back

Close

Full Screen / Esc

Printer-friendly Version

Interactive Discussion



1 Introduction

Biogenically emitted monoterpenes are important to atmospheric organic aerosol concentration and composition due to their large emission rates and high secondary organic aerosol (SOA) yields (Guenther et al., 1995; Hoffmann et al., 1997; Chung and Seinfeld, 2002; Pye et al., 2010). Of the monoterpenes, α -pinene is the most abundantly emitted. Many carboxylic acids, organonitrates, and organosulfates associated with α -pinene have been observed in aerosols both in the field and from laboratory oxidation (Kavouras et al., 1998, 1999; Yu et al., 1999b; Jaoui and Kamens, 2001; Larsen et al., 2001; Librando and Tringali, 2005; Surratt et al., 2007, 2008; Laaksonen et al., 2008; Zhang et al., 2010). A number of carboxylic acids have been used as particle-phase tracers of α -pinene oxidation, including pinonic acid, pinic acid, 10-hydroxypinonic acid, terpenylic acid, diaterpenylic acid acetate, and 3-methyl-1,2,3-butanetricarboxylic acid (3-MBTCA). For instance, pinonic and pinic acid have been observed to be in high concentration in aerosols collected in Portugal (accounting for 18–40 % of fine particle mass), in Greece (up to 26 % of fine particle mass), as well as in high yield in Finland (Kavouras et al., 1998, 1999; Anttila et al., 2005).

In the troposphere, α -pinene is oxidized approximately equally by OH and O_3 during the daytime (Capouet et al., 2008). During the nighttime, NO_3 is the most important oxidant of α -pinene worldwide and oxidation by NO_3 can be important during the daytime under conditions of elevated NO_x (Spittler et al., 2006). After reaction with the oxidant, the peroxy radicals that are formed can react with a number of species, including HO_2 , NO, NO_2 and other peroxy radicals (RO_2). Depending on the nature of the reactant with the peroxy radical, different oxidation products are produced in the gas phase. This was demonstrated in Part 1 of this series of papers (Eddingsaas et al., 2012). From a modeling standpoint, it is of interest to understand how the different gas-phase reaction mechanisms influence the particle-phase composition and concentration. This understanding will improve the ability to accurately simulate the amount of aerosol produced in the oxidation of α -pinene.

α -pinene photooxidation particle phase composition

N. C. Eddingsaas et al.

Title Page

Abstract

Introduction

Conclusions

References

Tables

Figures



Back

Close

Full Screen / Esc

Printer-friendly Version

Interactive Discussion



In this study, we describe the SOA yield and particle phase composition from the photooxidation of α -pinene under conditions where the peroxy radical chemistry is known. We focus on OH photooxidation because particle-phase composition from ozonolysis of α -pinene has been extensively studied (Glasius et al., 1999; Yu et al., 1999a; Iinuma et al., 2005; Presto et al., 2005; Ma et al., 2008; Shilling et al., 2009). The SOA composition from OH photooxidation has been much less studied and there are almost no studies examining low-NO_x conditions (Noziere et al., 1999; Ng et al., 2007a; Claeys et al., 2009). We discuss SOA composition focusing on several carboxylic acids which have been used as tracers of α -pinene oxidation. The formation of organosulfates and nitroxy organosulfates formed from α -pinene photooxidation is also addressed. We compare SOA composition based on different peroxy radical reactants as well as different aerosol seed (i.e. no seed, ammonium sulfate (AS) seed, and ammonium sulfate and sulfuric acid (AS + SA) seed). Finally, the effect of seed acidity on both the gas-phase and particle-phase composition is discussed.

2 Experimental

Photooxidation experiments of α -pinene and pinonaldehyde were performed in the Caltech dual 28 m³ Teflon chambers. Details of the chamber facilities have been described elsewhere (Cocker et al., 2001; Keywood et al., 2004). Prior to each run, the chamber was flushed for a minimum of 24 h with dry purified air. While being flushed, the chamber was irradiated with the chamber lights for a minimum of six hours. The temperature, relative humidity, and concentrations of O₃, NO, and NO_x (NO and NO₂) were continuously monitored. In all experiments the RH was kept below 10 %. Aerosol size distribution and number concentration were measured continuously by a differential mobility analyzer (DMA, TSI model 3081) coupled to a condensation nucleus counter (TSI model 3760). Aerosol growth data were corrected for size dependent wall-loss (Keywood et al., 2004; Ng et al., 2007b).

α -pinene photooxidation particle phase composition

N. C. Eddingsaas et al.

Title Page

Abstract

Introduction

Conclusions

References

Tables

Figures

⏪

⏩

◀

▶

Back

Close

Full Screen / Esc

Printer-friendly Version

Interactive Discussion



**α -pinene
photooxidation
particle phase
composition**

N. C. Eddingsaas et al.

Title Page

Abstract

Introduction

Conclusions

References

Tables

Figures

⏪

⏩

◀

▶

Back

Close

Full Screen / Esc

Printer-friendly Version

Interactive Discussion

Experiments were performed under low- and high-NO_x conditions. Under low-NO_x conditions, photolysis of hydrogen peroxide (H₂O₂) was the OH source, while for the high-NO_x experiments the photolysis of nitrous acid (HONO) or methyl nitrite (CH₃ONO) produced OH. For low-NO_x experiments, 280 μl of 50 wt% H₂O₂ was injected into the chamber resulting in a concentration ~4 ppm. Using HONO and CH₃ONO allowed the ratio of NO to NO₂ to be varied, with a lower ratio in the CH₃ONO experiments. For the remainder of this paper, the use of HONO as the OH source will be referred to as high-NO and the use of methyl nitrite will be referred to as high-NO₂ to distinguish between the relative importance of NO and NO₂.

HONO was prepared daily by dropwise addition of 15 ml of 1 wt% NaNO₂ into 30 ml of 10 wt% H₂SO₄ in a glass bulb, and then introduced into the chamber with dry air. This process produces NO and NO₂ as side products, which are also introduced to the chamber. CH₃ONO was synthesized, purified, and stored according to the procedure outlined by Taylor et al. (1980). CH₃ONO was warmed from liquid nitrogen temperatures and vaporized into an evacuated 500 ml glass bulb and introduced into the chamber with an air stream of 5 l min⁻¹. After addition of CH₃ONO, 300–400 ppb of NO was added to the chamber to suppress the formation of O₃. Determination of exact NO and NO₂ concentrations using the commercial NO_x monitor was precluded due to interferences by both HONO and CH₃ONO. At the start of all high-NO_x experiments the total NO_x reading (NO, NO_x, and interference from HONO or CH₃ONO) was 800 ppb and NO concentration throughout the experiments was such that the concentration of O₃ never exceeded 5 ppb.

Experiments were performed with either no aerosol seed present, ammonium sulfate seed (AS), or ammonium sulfate plus sulfuric acid (AS + SA). The AS + SA produced a much more acidic aerosol seed. When applicable, seed particles were added to the chamber after the addition of the oxidant. Aerosol seed particles were generated by atomizing an aqueous solution of 15 mM (NH₄)₂SO₄ (AS) or 15 mM (NH₄)₂SO₄ and 15 mM H₂SO₄ (AS + SA). Upon addition of an aerosol seed, the initial aerosol number

concentration was $\sim 1.8 \times 10^4 \text{ cm}^{-3}$, with a mean diameter of $\sim 60 \text{ nm}$, resulting in the initial aerosol volume of $10\text{--}15 \mu\text{m}^3 \text{ cm}^{-3}$.

Once the aerosol seed was added and stable, α -pinene was added to the chamber by transferring a known amount of α -pinene from a small glass bulb to achieve a concentration of 20–50 ppb. The mixing ratio of α -pinene was monitored with a gas chromatograph (Agilent 6890N) coupled with a flame ionization detector (GC-FID). The GC-FID was calibrated for α -pinene using a standard prepared in a 55 l Teflon bag.

Gas-phase photooxidation products were monitored by a custom-modified Varian 1200 triple-quadrupole chemical ionization mass spectrometer (CIMS) (St. Clair et al., 2010). Details of the operation of the CIMS can be found in a number of previous reports (Crouse et al., 2006; Paulot et al., 2009a; St. Clair et al., 2010). The CIMS was operated in negative ion mode using CF_3O^- as the reagent ion, and in the positive ion mode using H_3O^+ for proton transfer mass spectrometry (PTR-MS). In negative mode, CF_3O^- is sensitive to the detection of polar and acidic compounds by either clustering with the analyte (R) resulting in an ion with a mass-to-charge ratio (m/z) $\text{MW} + 85$ ($\text{R} \cdot \text{CF}_3\text{O}^-$) or via fluorine ion transfer resulting in m/z $\text{MW} + 19$ ($\text{HF} \cdot \text{R}_{-\text{H}}^-$). The dominant ionization mechanism depends mostly on the acidity of the neutral species; highly acidic species such as nitric acid form only the fluorine transfer ion, while non-acidic species such as methyl hydrogen peroxide form only the cluster ion. This separation aids both in the determination of the structure of a molecule and in the identification of isomers. In negative mode, tandem mass spectrometry (MS/MS) was used to help identify functional groups of an analyte. In brief, a parent ion selected in the first quadrupole is exposed to an elevated pressure of N_2 resulting in collision-induced dissociation (CID) in the second quadrupole, and the resulting fragmentation ions are detected in the third quadrupole. Molecules with different functional groups have been shown to fragment differently by CID. For example, fragmentation of hydroperoxides form a characteristic anion at m/z 63 (Paulot et al., 2009b). Unfortunately, authentic standards for most compounds described here are not readily available, and thus the sensitivity of the CIMS cannot be experimentally determined. In the absence of such

α -pinene photooxidation particle phase composition

N. C. Eddingsaas et al.

Title Page

Abstract

Introduction

Conclusions

References

Tables

Figures



Back

Close

Full Screen / Esc

Printer-friendly Version

Interactive Discussion

standards, we estimate that the sensitivity scales with the thermal capture rate and the binding energy of the cluster ($\text{VOC} \cdot \text{CF}_3\text{O}^-$). Details on calculating the sensitivity of the CIMS to a given analyte can be found in previous publications (Paulot et al., 2009a,b).

Duplicate Teflon filters (PALL Life Sciences, 47 mm diameter, 1.0 μm pore size, Teflon membrane) were collected from each of the chamber experiments for off-line chemical analysis. Filter sampling was started when the aerosol volume reached a constant value. For the chemical analysis, each filter was extracted with methanol (LC-MS CHROMASOLV-grade, Sigma-Aldrich) under ultrasonication for 45 min. The extract was dried under ultra-pure nitrogen gas, and the residue was reconstituted with a 50:50 (v/v) solvent mixture of methanol with 0.1 % acetic acid (LC-MS CHROMASOLV-grade, Sigma-Aldrich) and water with 0.1 % acetic acid (LC-MS CHROMASOLV-grade, Sigma-Aldrich). Filter sample extracts were analyzed by ultra-performance liquid chromatography/electrospray ionization-time-of-flight mass spectrometry (UPLC/ESI-TOFMS) operated in negative ion mode. Further details of the filter collection, sample preparation procedures, and UPLC/ESI-TOFMS analysis can be found in a previous publication (Surratt et al., 2008; Chan et al., 2010).

Products having either a carboxylic acid group or are organosulfates can be ionized via deprotonation and are detected in the negative ion mode as $[\text{M} - \text{H}]^-$ ions. All accurate mass measurements were within ± 5 mDa of the theoretical mass associated with the proposed chemical formula. From repeated UPLC/ESI-TOFMS measurements, the variations in the chromatographic peak areas are about 5 % (Chan et al., 2011). The concentrations are not corrected for extraction efficiencies.

High-resolution time-of-flight aerosol mass spectrometry (HR-ToF-AMS) spectra were obtained for one low- NO_x experiment with AS seed and one high- NO_x experiment with AS seed. The analysis of the data has previously been reported (Chhabra et al., 2011). Both high-resolution W-mode and higher sensitivity V-mode were taken, switching between the two modes every minute. The V-mode data were analyzed using a fragmentation table that enables separation of sulfate, ammonium, and organic components and to time-trace specific mass-to-charge ratios (m/z) (Allan et al., 2004).

α -pinene photooxidation particle phase composition

N. C. Eddingsaas et al.

Title Page

Abstract

Introduction

Conclusions

References

Tables

Figures

⏪

⏩

◀

▶

Back

Close

Full Screen / Esc

Printer-friendly Version

Interactive Discussion



W-mode data were analyzed using the high-resolution spectra toolbox, PIKA, to determine the chemical formulas contributing to distinct m/z (DeCarlo et al., 2006).

3 Results and discussion

In Part 1 (Eddingsaas et al., 2012), the gas-phase composition of OH photooxidation of α -pinene under low- NO_x , high-NO (HONO as the OH source), and high- NO_2 (methyl nitrite as the OH source) conditions was discussed. Under low- NO_x conditions, care was taken to ensure that reaction with HO_2 dominated the loss of the peroxy radicals. O_3 was suppressed in all experiments so that the oxidation of α -pinene was completely dominated by OH oxidation. Here, the results of the aerosol phase growth, yield, and composition from these controlled experiments are discussed.

3.1 Aerosol growth and yield

Table 1 lists the experimental conditions of the studies, the SOA yields, and a number of other variables of interest. The SOA density used to calculate SOA mass and SOA yield were taken from previous results: 1.32 g cm^{-3} under low- NO_x conditions and 1.33 g cm^{-3} under high- NO_x conditions (Ng et al., 2007a). SOA yield is calculated cumulatively throughout the experiments as the ratio of SOA mass to the mass of α -pinene reacted. For this suite of experiments, we cannot directly relate the time-dependent aerosol growth curves (i.e. SOA mass as a function of experiment time) to yield because the OH concentration varied widely between the systems. For example, the initial OH concentration for the low- NO_x experiments was $\sim 2 \times 10^6 \text{ molecules cm}^{-3}$, while in the high-NO experiments the initial OH was approximately 3 times larger, and under high- NO_2 conditions the initial OH was an order of magnitude larger, thereby resulting in much faster oxidation of α -pinene and faster aerosol growth. In addition, under both high-NO and high- NO_x conditions, the OH concentration declined significantly over time. The OH concentration through the experiments was determined by

α -pinene photooxidation particle phase composition

N. C. Eddingsaas et al.

Title Page

Abstract

Introduction

Conclusions

References

Tables

Figures

⏪

⏩

◀

▶

Back

Close

Full Screen / Esc

Printer-friendly Version

Interactive Discussion



**α -pinene
photooxidation
particle phase
composition**

N. C. Eddingsaas et al.

Title Page

Abstract

Introduction

Conclusions

References

Tables

Figures

⏪

⏩

◀

▶

Back

Close

Full Screen / Esc

Printer-friendly Version

Interactive Discussion

comparing the loss of α -pinene to a kinetic model of α -pinene OH oxidation under low- or high- NO_x conditions. Details of the model and gas phase measurements can be found in Part 1 (Eddingsaas et al., 2012). By using OH exposure (as units of OH concentration multiplied by reaction time in hours) as the coordinate system, a more direct comparison between different photooxidation systems is, however, possible.

Figure 1 shows SOA yield as a function of OH exposure from all experiments in the presence of AS seed particles. The overall yield was consistent between runs with the same OH source, but there is a systematic difference in SOA yield between the systems, decreasing as the concentration of NO increases. SOA growth under high- NO_2 conditions resembles low- NO_x SOA growth more than it does high-NO SOA growth, consistent with the hypothesis that reaction of the peroxy radicals with NO leads to reduced yields. Second, the SOA yield from high- NO_2 continued to increase after two α -pinene lifetimes. This is in contrast to the high-NO experiments where most of the aerosol growth is complete after one α -pinene lifetime. The SOA from low- NO_x photooxidation also continued to increase after two α -pinene lifetimes. This indicates that later generation oxidation products are important in determining the amount of SOA formed. As discussed in the gas-phase analysis (Eddingsaas et al., 2012), a distinct difference in the later generation oxidation products is the formation of carboxylic acids and peracids in the low- NO_x photooxidation. In the high- NO_2 cases, more PANs and nitric acid are formed compared to high-NO.

Illustrating that later generation oxidation products are important to SOA growth, the gas-phase time traces of first- and second-generation oxidation products are shown along with the SOA growth under all three conditions in the presence of ammonium sulfate seed in Fig. 2. Under all conditions, aerosol growth continues through the production of second-generation oxidation products. Under low- NO_x conditions, the signal for pinonaldehyde peracid and/or 10-hydroxypinonic acid is lost from the gas phase faster than pinonic acid. This is likely due to greater partitioning into the aerosol phase as a result of its lower vapor pressure. In the presence of high- NO_2 , pinonaldehyde PAN is observed to be lost from the gas phase faster than SOA growth as a result of

thermal decomposition. Pinonaldehyde nitrate is lost at a faster rate when methyl nitrite is the OH source. This could be due to either higher OH exposure or aerosol uptake.

The effect of the acidity of the seed particle on SOA yield was investigated. Figure 3 shows the SOA yield as a function of OH exposure with no seed, and in the presence of either AS seed (mildly acidic) or AS + SA seed (highly acidic) in low-NO_x, high-NO, and high-NO₂ OH oxidation. From low-NO_x photooxidation with initial α -pinene concentration of ~50 ppb, there is no difference in the aerosol growth in the presence of no, AS, or AS + SA seed. This was expected as the only difference in the gas-phase composition is that α -pinene oxide is in lower concentration in the presence of an acidic seed. α -pinene oxide is a minor product. This indicates that there is almost no reactive uptake occurring due to acid-catalyzed reactions and that if there are any changes in the aerosol composition, they occur within the particle phase. SOA yield was different when the initial α -pinene concentration was reduced to 20 ppb (37 % compared to 26–29 % when the initial concentration was 50 ppb). The cause of the increase in SOA yield with lower α -pinene concentration is not known.

As with low-NO_x photooxidation, there is no difference in aerosol growth under any seed conditions for high-NO₂ photooxidation. However, with high-NO, the yield does depend on seed conditions; yields increase from no seed to AS seed to AS + SA seed (increase of 22 % from AS to AS + SA seed). In the presence of AS + SA seed, the SOA yield is independent of NO₂ concentration. This small increase with acidity is in contrast to low-NO_x photooxidation of isoprene where the SOA increased markedly (1000 %) (Surratt et al., 2010).

Self-nucleation under high-NO conditions did not occur until nearly one α -pinene lifetime. In contrast, nucleation occurred nearly immediately under both high-NO₂ and low-NO_x conditions. One possible explanation for the difference in behavior is that for the aerosols in the presence of higher NO₂ case, the self-nucleated and AS seeded aerosols are more acidic than in the low-NO₂ case due to increased partitioning of nitric acid and possibly the PANs. This would result in an acidic aerosol under all conditions for the higher NO₂ experiments. When AS + SA seed is used, the particles have the

α -pinene photooxidation particle phase composition

N. C. Eddingsaas et al.

[Title Page](#)[Abstract](#)[Introduction](#)[Conclusions](#)[References](#)[Tables](#)[Figures](#)[Back](#)[Close](#)[Full Screen / Esc](#)[Printer-friendly Version](#)[Interactive Discussion](#)

same level of acidity and partitioning should be more similar. Analysis of the particle-phase composition provides more insight into the differences between the systems.

3.2 Aerosol chemical composition

Tables 2 and 3 list the UPLC peak areas for each of the carboxylic acids associated with atmospheric photooxidation of α -pinene under low-NO_x, high-NO, and high-NO₂ conditions, in the presence of either AS or AS + SA seed. The peak areas are presented both as the raw peak areas (Table 2) as well as peak areas scaled to the SOA mass load of the low-NO_x AS seed run (Table 3), so that a weighted average of each component can be compared. Concentration calibrations were not performed and therefore the analysis is qualitative. Figure 4 shows the UPLC chromatograms from the filter samples from low-NO_x OH oxidation in the presence of AS or AS + SA seed particles along with the chromatogram from pinonaldehyde low-NO_x photooxidation, while Fig. 5 shows the UPLC chromatograms from high-NO and high-NO₂ OH oxidation in the presence of AS or AS + SA seed particles. The species of interest – pinonic acid, 10-hydroxy pinonic acid, pinic acid, terpenylic acid, 2-hydroxy terpenylic acid, diaterpenylic acid acetate, 3-MBTCA, the organosulfates and the nitrooxy organosulfates have previously been identified by UPLC/(-)ESI-TOFMS (Warnke et al., 2006; Szmigielski et al., 2007; Claeys et al., 2009), and it is these identifications that are being used to confirm the presence or absence of each species.

Pinonic acid, pinic acid, and 10-hydroxy pinonic acid are only observed in substantial quantities in the aerosol phase from the low-NO_x photooxidation (Tables 2 and 3 and Fig. 4). This was expected as pinonic and 10-hydroxy pinonic acid were only observed in the gas-phase in the low-NO_x photooxidation (Eddingsaas et al., 2012). These species originate from the oxidation of pinonaldehyde as confirmed by the gas-phase data (Eddingsaas et al., 2012) as well as the UPLC chromatogram of the low-NO_x photooxidation of pinonaldehyde (Fig. 4c). Pinonic acid, pinic acid, and 10-hydroxy pinonic acid are also typical species found in SOA from the ozonolysis of α -pinene (Hoffmann et al., 1997; Ma et al., 2008; Camredon et al., 2010). Thus, it is likely that

α -pinene photooxidation particle phase composition

N. C. Eddingsaas et al.

Title Page

Abstract

Introduction

Conclusions

References

Tables

Figures



Back

Close

Full Screen / Esc

Printer-friendly Version

Interactive Discussion



previous observation of pinonic acid, pinic acid, and 10-hydroxy pinonic acid in studies of α -pinene high-NO_x photooxidation were a result of ozonolysis and not OH chemistry.

3-MBTCA is believed to be a tracer compound of α -pinene derived SOA (Szmigielski et al., 2007; Kourtchev et al., 2009; Zhang et al., 2010) and indeed it was observed here under all conditions (as well as from the low-NO_x photooxidation of pinonaldehyde). It has been proposed that 3-MBTCA is the result of further high-NO_x oxidation of pinonic acid in the gas phase (Szmigielski et al., 2007; Müller et al., 2012). While a recent study by Müller et al. (2012) shows evidence of gas-phase formation of 3-MBTCA from the photooxidation of pinonic acid in the presence of NO, other reaction pathways for the formation of 3-MBTCA must exist, because, in the present study, 3-MBTCA is observed under high-NO and high-NO₂ conditions when pinonic acid is not observed and, in addition, 3-MBTCA is observed from low-NO_x photooxidation where peroxy radical reactions are dominated by reactions with HO₂. The ratio of 3-MBTCA to pinic acid in low-NO_x oxidation of α -pinene is substantially greater than from pinonaldehyde photooxidation. This is in contrast to the ratios of pinic acid, pinonic acid, and 10-hydroxypinonic acids which are very similar regardless of which initial hydrocarbon was used under low-NO_x conditions.

Terpenylic acid and diaterpenylic acid were observed in filters from all α -pinene photooxidation mechanisms, while 2-hydroxy terpenylic acid was observed only in the presence of NO. Under low-NO_x photooxidation, terpenylic acid is the dominant peak and is observed only as a dimer (m/z 343), while diaterpenylic acid is a minor peak. In the low-NO_x photooxidation of pinonaldehyde, terpenylic acid was observed, but it is a small contributor to the aerosol mass; diaterpenylic acid was not observed at all. There is a peak in the chromatograms for low-NO_x photooxidation of α -pinene and pinonaldehyde with a molecular ion that corresponds to 2-hydroxy terpenylic acid (m/z = 187.06), but it elutes much earlier than found in previous studies (Claeys et al., 2009) or in the high-NO or high-NO₂ studies here. Under high-NO and high-NO₂ photooxidation, diaterpenylic acid acetate is observed to be the dominant peak in the chromatograms. Terpenylic and 10-hydroxy terpenylic acids are also dominant peaks in the

α -pinene photooxidation particle phase composition

N. C. Eddingsaas et al.

Title Page

Abstract

Introduction

Conclusions

References

Tables

Figures

⏪

⏩

◀

▶

Back

Close

Full Screen / Esc

Printer-friendly Version

Interactive Discussion

chromatograms, with their contribution to the total aerosol greater with higher NO_2 . From this analysis, it appears that terpenylic acid arises from the photooxidation of pinonaldehyde while diaterpenylic acid acetate is from some other channel of α -pinene photooxidation.

5 The composition of the SOA in low- NO_x photooxidation in the presence of AS or AS + SA seed is very similar (see Tables 2 and 3 and Fig. 4). This is consistent with the fact that the SOA yield and mass loading were almost identical between these experiments. In the presence of the acidic seed, four peaks were observed that correspond to organosulfates, one with m/z 279 and three with m/z 249. The organosulfate peak at
10 m/z 279 has been previously identified as the sulfate ester of 10-hydroxy pinonic acid and is thought to originate from the esterification of the hydroxyl group of 10-hydroxy pinonic acid (Surratt et al., 2008). Indeed, the signal for 10-hydroxy pinonic acid decreases in the presence of AS + SA seed (Table 3), while no change in peak area is observed from either pinonic or pinic acid, both of which lack a hydroxyl group. While
15 it has been shown that for simple alcohols, sulfate esterification is too slow to be atmospherically relevant (Minerath et al., 2008), these data indicate that esterification may be sufficiently fast in more complex, acidic alcohols. The three peaks with m/z 249 are most likely from the reactive uptake of α -pinene oxide, which was observed to be in lower concentration in the gas phase in the presence of an acidic seed. Iinuma
20 et al. (2009) have shown that the uptake of α -pinene oxide results in the formation of three different organosulfates: 2-pinanol-3-hydrogen sulfate, 3-pinanol-2-hydrogen sulfate, and campholenol hydrogen sulfate. The SOA yield is independent of aerosol seed acidity from low- NO_x photooxidation indicating that the gas-phase yield of α -pinene oxide and the resulting organosulfates are minor components.

25 The SOA composition (and yield) from high- NO photooxidation is substantially different in the presence of AS + SA seed. In the presence of an acidic seed, diaterpenylic acid and 2-hydroxy terpenylic acid were greatly reduced in the aerosol while terpenylic acid was relatively unchanged (see Tables 2 and 3 and Fig. 5). A large number of organosulfates and nitroxy organosulfates are observed. Both of the organosulfates

α -pinene photooxidation particle phase composition

N. C. Eddingsaas et al.

Title Page

Abstract

Introduction

Conclusions

References

Tables

Figures

⏪

⏩

◀

▶

Back

Close

Full Screen / Esc

Printer-friendly Version

Interactive Discussion

observed in low-NO_x photooxidation are observed. The source of the *m/z* 249 is most likely the same, α -pinene oxide. The mechanism for the formation of the sulfate ester of 10-hydroxy pinonic acid is less clear. 10-hydroxy pinonic acid is not observed in the gas phase, is a small fraction of the particle phase mass, and its aerosol concentration is relatively unchanged in the presence of an acidic seed. In addition, 10-hydroxy pinonic acid is more prominent in low-NO_x photooxidation. However, the organosulfate associated with 10-hydroxy pinonic acid is of greater abundance in high-NO and high-NO₂ conditions than in low-NO_x conditions. The sulfate ester of 10-hydroxy pinonic acid coelutes with two other ions and therefore the peak area has greater error. However, even if the peak areas were similar, it would not be consistent with a source from 10-hydroxy pinonic acid under high-NO and high-NO₂ conditions due to the low signal. The peak is observed at the same chromatographic time under all conditions; therefore, either the organosulfates at *m/z* 279 are formed by different processes depending on NO concentration, or 10-hydroxy pinonic acid is not the source at all. We believe that there must be another mechanism that forms this organosulfate. The nitrooxy organosulfate (*m/z* = 310) elutes as two peaks in the chromatogram. Under high-NO and high-NO₂ conditions, a species is formed in the gas phase with molecular weight of 231 (CIMS *m/z* = 316). This gas-phase species was assigned to α -pinene dihydroxy nitrate as proposed in previous reports and upon sulfate esterification would produce a nitrooxy organosulfate that would produce the ion of interest (*m/z* 310) (Aschmann et al., 2002; Surratt et al., 2008). Thus, there is once again evidence for particle-phase sulfate esterification of a hydroxyl group in a poly-functional molecule. The largest sulfate peak was also the dominant peak in the chromatogram corresponding to *m/z* 247. The identification of the compound is unknown and its overall importance to the SOA yield is not known as no calibrations are available. Tables 2 and 3 list the most likely molecular formula for the ion at *m/z* 247, along with those from the other observed organosulfates and nitrooxy organosulfates.

Under high-NO₂ conditions, the addition of AS + SA rather than AS seed results in fewer new peaks in the UPLC chromatogram than under high-NO conditions. As with

α -pinene photooxidation particle phase composition

N. C. Eddingsaas et al.

Title Page

Abstract

Introduction

Conclusions

References

Tables

Figures



Back

Close

Full Screen / Esc

Printer-friendly Version

Interactive Discussion

low-NO_x, this result is expected as the SOA yield is insensitive to aerosol acidity. As with high-NO, 2-hydroxy terpenylic acid decreases in concentration in the presence of an acidic seed; however, the concentration of diaterpenylic acid acetate, the presumed precursor, is insensitive to aerosol acidity. We have no explanation for this discrepancy. All of the organosulfates and nitrooxy organosulfates observed in high-NO₂ photooxidation are observed in high-NO photooxidation, but there are a few additional organosulfates and nitrooxy organosulfates that are unique to the high-NO case (see Tables 2 and 3 and Fig. 5).

Given that the SOA yield and growth curves are so different, it is surprising that the UPLC/(-)ESI-TOFMS data from high-NO or high-NO₂ photooxidation are remarkably similar in the presence of AS seed but substantially different with AS + SA seed (see Fig. 5). This suggests that there must be compositional differences which UPLC/(-)ESI-TOFMS is insensitive. The data also suggest that PANs may play a role in the SOA composition as the amount of PAN was the main difference observed in the gas phase.

The aerosol composition in low-NO_x and high-NO₂ OH oxidation of α -pinene in the presence of AS seed particles was further analyzed by HR-ToF-AMS. A description of the results has previously been reported (Chhabra et al., 2011). In Chhabra et al. (2011) the H:C vs O:C (Van Krevelen diagram) and the ratio of f_{44} (more oxidized species, CO₂⁺ likely from acids) to f_{43} (less oxidized species, C₂H₃O⁺) are compared over the course of the photooxidation experiments. The Van Krevelen diagram can be used to infer the bulk functionality of the organic species within the aerosol. Both the low-NO_x and high-NO₂ photooxidation of α -pinene fall along the -1 slope of the H:C vs. O:C plot (see Fig. 2 of Chhabra et al., 2011), a value indicative of either carboxylic acids and/or hydroxy carbonyls (Heald et al., 2010; Ng et al., 2011; Chhabra et al., 2011). Under both low-NO_x and high-NO₂ OH oxidation, the AMS data indicate the same bulk organic functionality while the gas-phase data show a greater quantity of carboxylic acids in the low-NO_x oxidation. Consistent with the Van Krevelen diagram, f_{44} to f_{43} is very similar between the low-NO_x and high-NO₂ experiments. f_{44} is assigned as an indicator of carboxylic acids and a higher degree of aerosol aging (Ng

α -pinene photooxidation particle phase composition

N. C. Eddingsaas et al.

Title Page

Abstract

Introduction

Conclusions

References

Tables

Figures

⏪

⏩

◀

▶

Back

Close

Full Screen / Esc

Printer-friendly Version

Interactive Discussion

et al., 2011; Chhabra et al., 2011). Further analysis of AMS data indicates that carboxylic acids are a large fraction (30–40 % of the mass) of the aerosols in low-NO_x and high-NO₂ OH oxidation of α -pinene (see Table 2 of Chhabra et al., 2011).

3.3 Gas-phase composition with injection of inorganic seed after photooxidation

To study how different oxidation products interact with aerosol seed particles of different composition (acidity), experiments were performed in which α -pinene was first photooxidized, followed by introduction of an aerosol seed after the lights had been off for two hours. This results in the exposure of gas-phase compounds, formed later on in the experiment, to fresh inorganic aerosol seed particles. This type of experiment has been used previously to study the SOA produced in the low-NO_x photooxidation of isoprene (Surratt et al., 2010). Surratt et al. (2010) showed that epoxydiols formed from the photooxidation of isoprene preferentially partition to acidic aerosol by reactive uptake.

Two post-oxidation seed experiments were performed under low-NO_x and two under high-NO₂ conditions. In all experiments, aerosol self-nucleation occurred as soon as the lights were turned on so a substantial amount of aerosol had already formed. Once the oxidation products were formed, the lights were extinguished and the chamber was left in the dark for two hours followed by injection of 15–20 $\mu\text{g m}^{-3}$ of aerosol seed. For low-NO_x, this added about 50 % more aerosol volume into the chamber, while for high-NO₂ the aerosol concentration was doubled.

Figure 6 shows the aerosol growth from each of the photooxidation followed by aerosol injection experiments. Aerosol nucleation and growth occurs as soon as the lights are turned on in all experiments. Once the lights are turned off, the aerosol mass remains constant until the addition of the inorganic seed. In the case of low-NO_x, an additional growth of $\sim 8 \mu\text{g m}^{-3}$ of SOA is observed after the addition of AS + SA seed; no growth is observed after the addition of the neutral seed. The difference in the aerosol growth is in contrast to the SOA behavior when the aerosol seed was added

α -pinene photooxidation particle phase composition

N. C. Eddingsaas et al.

Title Page

Abstract

Introduction

Conclusions

References

Tables

Figures

⏪

⏩

◀

▶

Back

Close

Full Screen / Esc

Printer-friendly Version

Interactive Discussion



prior to photooxidation. Under high-NO₂ conditions, no additional SOA is formed after the addition of either neutral or acidic seed particles in the dark.

When a neutral seed was added in the dark after photooxidation under low-NO_x or high-NO₂ conditions, no change in any of the gas-phase concentrations was observed.

This indicates that the gas-phase molecules were not simply in equilibrium with the total aerosol concentration. It is possible that the gas-phase species were partitioning to the wall as well as to the particles, and were at equilibrium; since the surface area of the chamber walls is two orders of magnitude larger than that of the aerosol, no loss would be observed simply due to the greater surface area. Equilibrium partitioning to the walls does not, however, seem likely as the concentration of nearly all the species in the gas phase did not change when the lights were extinguished, decreasing temperature of ~5 °C. If the gas-phase molecules were partitioning to the wall, it would be expected that their gas-phase concentration would drop as the temperature decreased.

The gas-phase concentration of a number of oxidation products formed under low-NO_x conditions were noticeably reduced when AS + SA seed particles were introduced after photooxidation (Fig. 7). α -pinene oxide is almost completely lost from the gas phase after introduction of the acidic seed (Fig. 7d). In addition, the highly oxidized products observed at *m/z* 301 and 303 decrease by ~70%. These two compounds probably contain either two hydroperoxy groups or one hydroperoxy group and one bridging peroxy group. Upon addition of the acidic aerosol seed, α -pinene hydroxy hydroperoxide also decreased from the gas phase by ~75% (Fig. 7a). This was unexpected, as it has been shown that the hydroxy hydroperoxides formed in the photooxidation of isoprene are not lost from the gas phase (Surratt et al., 2010). In addition, it was unexpected because when aerosol seed was added prior to photooxidation, the only gas-phase product observed to be in lower concentration in the presence of a highly acidic seed was α -pinene oxide. It should be noted that the gas-phase mass loss was a factor of two greater than the SOA growth upon addition of AS + SA seed. It is not clear how to interpret the mass balance, as no species were observed to increase substantially in the gas phase after addition of the acidic seed.

α -pinene photooxidation particle phase composition

N. C. Eddingsaas et al.

[Title Page](#)[Abstract](#)[Introduction](#)[Conclusions](#)[References](#)[Tables](#)[Figures](#)[⏪](#)[⏩](#)[◀](#)[▶](#)[Back](#)[Close](#)[Full Screen / Esc](#)[Printer-friendly Version](#)[Interactive Discussion](#)

The loss of additional organics upon addition of AS + SA seed after photooxidation compared to when the seed is injected prior to photooxidation may be related to the composition of the seed when exposed to a given organic. Specifically, perhaps products that are involved in self-nucleation and partition early on in the experiment coat the acidic seed resulting in a hydrocarbon surface rather than an acidic one. If this is the case, loss to the particle would be due to hydrocarbon partitioning rather than acid-catalyzed reactive uptake. Aerosol growth occurs as soon as the lights are turned on, and when a seed is present it takes only about 1.25 h before the aerosol volume has doubled. On the other hand, when the acidic seed is injected after photooxidation has occurred, the products are exposed to the acidic surface allowing reactive uptake to occur from the accumulated products. If this is the case, SOA yield from α -pinene photooxidation from laboratory experiments might underestimate the effect of an acidic aerosol. More studies are needed to determine if this is the case as well as to see what new species would be observed in the particle phase.

Under high-NO₂ conditions, α -pinene oxide is substantially lost from the gas phase when the acidic seed was added (Fig. 8). Besides α -pinene oxide, there are minimal losses of other gas-phase species (Fig. 8). The observed losses include compounds that show up at m/z 215, 301, and 316. The loss of each of these is less than 25 %, as opposed to the low-NO_x case where losses were all greater than 50 %. As mentioned above, multiple species are observed at m/z 316, a product from the oxidation of α -pinene and norpinonaldehyde PAN. It is expected that if norpinonaldehyde PAN were to be lost from the gas phase upon addition of an acidic seed then pinonaldehyde PAN would as well. There is no loss of pinonaldehyde PAN from the gas phase, and therefore we conclude that the species lost from the gas phase is the α -pinene oxidation product, which we believe to be α -pinene dihydroxy nitrate. The structures of the molecules at m/z 215 and 301 are not known. Due to the small losses, it appears that under high-NO₂ conditions, acidity will play only a small or negligible effect on SOA growth, as seen in Fig. 6 where no additional growth was observed upon addition of an acidic seed. Consistent with this result, Offenberg et al. (2009) saw only a modest increase

α -pinene photooxidation particle phase composition

N. C. Eddingsaas et al.

[Title Page](#)[Abstract](#)[Introduction](#)[Conclusions](#)[References](#)[Tables](#)[Figures](#)[⏪](#)[⏩](#)[◀](#)[▶](#)[Back](#)[Close](#)[Full Screen / Esc](#)[Printer-friendly Version](#)[Interactive Discussion](#)

in SOA yield with the increase of the aerosol acidity from high-NO₂ photooxidation of α -pinene.

4 Implications

In this study, the aerosol growth and composition from α -pinene OH oxidation were compared in low-NO (RO₂ + HO₂) and high-NO (RO₂ + NO) conditions. Aerosol growth from α -pinene OH oxidation under high-NO₂ conditions behaves more similarly to low-NO_x than high-NO aerosol growth. With low NO, aerosol growth continues well after two lifetime of α -pinene with respect to OH oxidation. This indicates that later generation oxidation products are important for SOA growth, including the products of the oxidation of pinonaldehyde, a major product of both low- and high-NO OH oxidation of α -pinene.

In high-NO conditions the SOA yield is dependent on aerosol acidity. The increase in SOA yield with acidic seed was, however, relatively small (~22% increase). The composition of the gas phase between high-NO and high-NO₂ OH oxidation was identical with a few notable variations. In the presence of elevated NO₂ levels, greater concentrations of PANs and nitric acid were observed in the gas phase. One possible explanation for the difference in SOA growth is that the aerosols formed under high-NO₂ conditions are acidic enough in the presence of a neutral seed, due to the increased nitric acid and PANs, for the SOA yield to be the same in the presence of neutral or acidic particles. Further studies on the effect of NO₂, PANs, and nitric acid on SOA yield from high-NO_x OH oxidation of α -pinene would aid in elucidating the difference in behavior between using HONO and methyl nitrite as the OH source.

When an acidic seed was added after OH oxidation, the SOA yield under low-NO_x conditions increased with a corresponding loss of species from the gas phase. This acid effect was not observed when the aerosol seed is added prior to oxidation, perhaps due to differences in the composition of the aerosol surface. The hypothesis is that when aerosol seed particles are added prior to oxidation, the surface is coated by organics, suppressing uptake of compounds that are catalyzed by acid. This has

α -pinene photooxidation particle phase composition

N. C. Eddingsaas et al.

Title Page

Abstract

Introduction

Conclusions

References

Tables

Figures

⏪

⏩

◀

▶

Back

Close

Full Screen / Esc

Printer-friendly Version

Interactive Discussion



potential implications to any system that produces a high SOA yield or systems that start with a high organic VOC concentration. In systems where the seed particles become coated with organics relatively quickly, the acid effect and therefore the SOA yield under acidic conditions might be under represented.

Organic acids are a major component of SOA in both low- and high-NO_x OH oxidation of α -pinene. While AMS data indicate that the total concentration of organic acids in SOA from low-NO_x and high-NO₂ is similar, the individual composition varies depending on the gas-phase conditions. Pinonic and pinic acid are observed in SOA only from low-NO_x OH oxidation of α -pinene. This is consistent with gas-phase data, where pinonic acid was only observed from low-NO_x conditions. It is believed that 3-MBTCA is derived from high-NO_x gas phase oxidation of pinonic acid; however, there must be other mechanism for its formation, as 3-MBTCA is observed in SOA from low-NO_x OH oxidation of α -pinene and high-NO_x OH oxidation of α -pinene where pinonic acid is not observed in the gas or aerosol phase.

Acknowledgements. This work was supported in part by Department of Energy grant DE-SC0006626 and National Science Foundation grant AGS-1057183. N. Eddingsaas was supported by the Camille and Henry Dreyfus Postdoctoral Program in Environmental Chemistry. C. Loza and L. Yee were supported by National Science Foundation Graduate Research Fellowships.

References

Allan, J. D., Delia, A. E., Coe, H., Bower, K. N., Alfarra, M. R., Jimenez, J. L., Middlebrook, A. M., Drewnick, F., Onasch, T. B., Canagaratna, M. R., Jayne, J. T., and Worsnop, D. R.: A generalised method for the extraction of chemically resolved mass spectra from aerodyne aerosol mass spectrometer data, *J. Aerosol Sci.*, 35, 909–922, doi:10.1016/j.jaerosci.2004.02.007, 2004. 8585

Anttila, P., Hyotylainen, T., Heikkilä, A., Jussila, M., Finell, J., Kulmala, M., and Riekkola, M. L.: Determination of organic acids in aerosol particles from a coniferous forest by liquid

α -pinene photooxidation particle phase composition

N. C. Eddingsaas et al.

Title Page

Abstract

Introduction

Conclusions

References

Tables

Figures



Back

Close

Full Screen / Esc

Printer-friendly Version

Interactive Discussion



**α -pinene
photooxidation
particle phase
composition**

N. C. Eddingsaas et al.

Title Page

Abstract

Introduction

Conclusions

References

Tables

Figures



Back

Close

Full Screen / Esc

Printer-friendly Version

Interactive Discussion

chromatography-mass spectrometry, *J. Sep. Sci.*, 28, 337–346, doi:10.1002/jssc.200401931, 2005. 8581

Aschmann, S. M., Atkinson, R., and Arey, J.: Products of reaction of OH radicals with alpha-pinene, *J. Geophys. Res.-Atmos.*, 107, 4191, doi:10.1029/2001jd001098, 2002. 8592

5 Camredon, M., Hamilton, J. F., Alam, M. S., Wyche, K. P., Carr, T., White, I. R., Monks, P. S., Rickard, A. R., and Bloss, W. J.: Distribution of gaseous and particulate organic composition during dark α -pinene ozonolysis, *Atmos. Chem. Phys.*, 10, 2893–2917, doi:10.5194/acp-10-2893-2010, 2010. 8589

10 Capouet, M., Mueller, J. F., Ceulemans, K., Compernelle, S., Vereecken, L., and Peeters, J.: Modeling aerosol formation in alpha-pinene photo-oxidation experiments, *J. Geophys. Res.-Atmos.*, 113, D02308, doi:10.1029/2007JD008995, 2008. 8581

Chan, M. N., Surratt, J. D., Claeys, M., Edgerton, E. S., Tanner, R. L., Shaw, S. L., Zheng, M., Knipping, E. M., Eddingsaas, N. C., Wennberg, P. O., and Seinfeld, J. H.: Characterization and Quantification of Isoprene-Derived Epoxydiols in Ambient Aerosol in the Southeastern United States, *Environ. Sci. Technol.*, 44, 4590–4596, doi:10.1021/es100596b, 2010. 8585

15 Chan, M. N., Surratt, J. D., Chan, A. W. H., Schilling, K., Offenberg, J. H., Lewandowski, M., Edney, E. O., Kleindienst, T. E., Jaoui, M., Edgerton, E. S., Tanner, R. L., Shaw, S. L., Zheng, M., Knipping, E. M., and Seinfeld, J. H.: Influence of aerosol acidity on the chemical composition of secondary organic aerosol from β -caryophyllene, *Atmos. Chem. Phys.*, 11, 1735–1751, doi:10.5194/acp-11-1735-2011, 2011. 8585

20 Chhabra, P. S., Ng, N. L., Canagaratna, M. R., Corrigan, A. L., Russell, L. M., Worsnop, D. R., Flagan, R. C., and Seinfeld, J. H.: Elemental composition and oxidation of chamber organic aerosol, *Atmos. Chem. Phys.*, 11, 8827–8845, doi:10.5194/acp-11-8827-2011, 2011. 8585, 8593, 8594

25 Chung, S. H. and Seinfeld, J. H.: Global distribution and climate forcing of carbonaceous aerosols, *J. Geophys. Res.-Atmos.*, 107, 4407, doi:10.1029/2001JD001397, 2002. 8581

30 Claeys, M., Iinuma, Y., Szmigielski, R., Surratt, J. D., Blockhuys, F., Van Alsenoy, C., Boge, O., Sierau, B., Gomez-Gonzalez, Y., Vermeylen, R., Van der Veken, P., Shahgholi, M., Chan, A. W. H., Herrmann, H., Seinfeld, J. H., and Maenhaut, W.: Terpenylic Acid and Related Compounds from the Oxidation of alpha-Pinene: Implications for New Particle Formation and Growth above Forests, *Environ. Sci. Technol.*, 43, 6976–6982, doi:10.1021/es9007596, 2009. 8582, 8589, 8590

**α -pinene
photooxidation
particle phase
composition**

N. C. Eddingsaas et al.

Title Page

Abstract

Introduction

Conclusions

References

Tables

Figures

⏪

⏩

◀

▶

Back

Close

Full Screen / Esc

Printer-friendly Version

Interactive Discussion



- Cocker, David R., I., Flagan, R. C., and Seinfeld, J. H.: State-of-the-art chamber facility for studying atmospheric aerosol chemistry, *Environ. Sci. Technol.*, 35, 2594–2601, 2001. 8582
- Crouse, J. D., McKinney, K. A., Kwan, A. J., and Wennberg, P. O.: Measurement of gas-phase hydroperoxides by chemical ionization mass spectrometry, *Anal. Chem.*, 78, 6726–6732, 2006. 8584
- 5 DeCarlo, P. F., Kimmel, J. R., Trimborn, A., Northway, M. J., Jayne, J. T., Aiken, A. C., Gonin, M., Fuhrer, K., Horvath, T., Docherty, K. S., Worsnop, D. R., and Jimenez, J. L.: Field-deployable, high-resolution, time-of-flight aerosol mass spectrometer, *Anal. Chem.*, 78, 8281–8289, doi:10.1021/ac061249n, 2006. 8586
- 10 Eddingsaas, N. C., Loza, C. L., Yee, L. D., Seinfeld, J. H., and Wennberg, P. O.: α -pinene photooxidation under controlled chemical conditions – Part 1: Gas-phase composition in low- and high-NO_x environments, *Atmos. Chem. Phys. Discuss.*, 12, 6447–6483, doi:10.5194/acpd-12-6447-2012, 2012. 8581, 8586, 8587, 8589
- 15 Glasius, M., Duane, M., and Larsen, B. R.: Determination of polar terpene oxidation products in aerosols by liquid chromatography-ion trap mass spectrometry, *J. Chromatogr. A*, 833, 121–135, 1999. 8582
- Guenther, A., Hewitt, C. N., Erickson, D., Fall, R., Geron, C., Graedel, T., Harley, P., Klinger, L., Lerdau, M., McKay, W. A., Pierce, T., Scholes, B., Steinbrecher, R., Tallamraju, R., Taylor, J., and Zimmerman, P.: A global model of natural volatile organic compound emissions, *J. Geophys. Res.-Atmos.*, 100, 8873–92, 1995. 8581
- 20 Heald, C. L., Kroll, J. H., Jimenez, J. L., Docherty, K. S., DeCarlo, P. F., Aiken, A. C., Chen, Q., Martin, S. T., Farmer, D. K., and Artaxo, P.: A simplified description of the evolution of organic aerosol composition in the atmosphere, *Geophys. Res. Lett.*, 37, L08803, doi:10.1029/2010gl042737, 2010. 8593
- 25 Hoffmann, T., Odum, J. R., Bowman, F., Collins, D., Klockow, D., Flagan, R. C., and Seinfeld, J. H.: Formation of organic aerosols from the oxidation of biogenic hydrocarbons, *J. Atmos. Chem.*, 26, 189–222, 1997. 8581, 8589
- Iinuma, Y., Boge, O., Miao, Y., Sierau, B., Gnauk, T., and Herrmann, H.: Laboratory studies on secondary organic aerosol formation from terpenes, *Faraday Discuss.*, 130, 279–294, doi:10.1039/b502160j, 2005. 8582
- 30 Iinuma, Y., Boge, O., Kahnt, A., and Herrmann, H.: Laboratory chamber studies on the formation of organosulfates from reactive uptake of monoterpene oxides, *Phys. Chem. Chem. Phys.*, 11, 7985–97, 2009. 8591

**α -pinene
photooxidation
particle phase
composition**

N. C. Eddingsaas et al.

Title Page

Abstract

Introduction

Conclusions

References

Tables

Figures

⏪

⏩

◀

▶

Back

Close

Full Screen / Esc

Printer-friendly Version

Interactive Discussion



Jaoui, M. and Kamens, R. M.: Mass balance of gaseous and particulate products analysis from alpha-pinene/NOx/air in the presence of natural sunlight, *J. Geophys. Res.-Atmos.*, 106, 12541–12558, 2001. 8581

Kavouras, I. G., Mihalopoulos, N., and Stephanou, E. G.: Formation of atmospheric particles from organic acids produced by forests, *Nature*, 395, 683–686, 1998. 8581

Kavouras, I. G., Mihalopoulos, N., and Stephanou, E. G.: Formation and gas/particle partitioning of monoterpenes photo-oxidation products over forests, *Geophys. Res. Lett.*, 26, 55–58, 1999. 8581

Keywood, M. D., Varutbangkul, V., Bahreini, R., Flagan, R. C., and Seinfeld, J. H.: Secondary organic aerosol formation from the ozonolysis of cycloalkenes and related compounds, *Environ. Sci. Technol.*, 38, 4157–4164, 2004. 8582

Kourtchev, I., Copolovici, L., Claeys, M., and Maenhaut, W.: Characterization of Atmospheric Aerosols at a Forested Site in Central Europe, *Environ. Sci. Technol.*, 43, 4665–4671, doi:10.1021/es803055w, 2009. 8590

Laaksonen, A., Kulmala, M., O'Dowd, C. D., Joutsensaari, J., Vaattovaara, P., Mikkonen, S., Lehtinen, K. E. J., Sogacheva, L., Dal Maso, M., Aalto, P., Petäjä, T., Sogachev, A., Yoon, Y. J., Lihavainen, H., Nilsson, D., Facchini, M. C., Cavalli, F., Fuzzi, S., Hoffmann, T., Arnold, F., Hanke, M., Sellegri, K., Umann, B., Junkermann, W., Coe, H., Allan, J. D., Alfarra, M. R., Worsnop, D. R., Riekkola, M. -L., Hyötyläinen, T., and Viisanen, Y.: The role of VOC oxidation products in continental new particle formation, *Atmos. Chem. Phys.*, 8, 2657–2665, doi:10.5194/acp-8-2657-2008, 2008. 8581

Larsen, B. R., Di Bella, D., Glasius, M., Winterhalter, R., Jensen, N. R., and Hjorth, J.: Gas-phase OH oxidation of monoterpenes: Gaseous and particulate products, *J. Atmos. Chem.*, 38, 231–276, 2001. 8581

Librando, V. and Tringali, G.: Atmospheric fate of OH initiated oxidation of terpenes. Reaction mechanism of alpha-pinene degradation and secondary organic aerosol formation, *J. Environ. Manag.*, 75, 275–282, doi:10.1016/j.jenvman.2005.01.001, 2005. 8581

Ma, Y., Russell, A. T., and Marston, G.: Mechanisms for the formation of secondary organic aerosol components from the gas-phase ozonolysis of alpha-pinene, *Phys. Chem. Chem. Phys.*, 10, 4294–4312, doi:10.1039/b803283a, 2008. 8582, 8589

Minerath, E. C., Casale, M. T., and Elrod, M. J.: Kinetics Feasibility Study of Alcohol Sulfate Esterification Reactions in Tropospheric Aerosols, *Environ. Sci. Technol.*, 42, 4410–4415, 2008. 8591

**α -pinene
photooxidation
particle phase
composition**

N. C. Eddingsaas et al.

Title Page

Abstract

Introduction

Conclusions

References

Tables

Figures

⏪

⏩

◀

▶

Back

Close

Full Screen / Esc

Printer-friendly Version

Interactive Discussion



- Müller, L., Reinnig, M.-C., Naumann, K. H., Saathoff, H., Mentel, T. F., Donahue, N. M., and Hoffmann, T.: Formation of 3-methyl-1,2,3-butanetricarboxylic acid via gas phase oxidation of pinonic acid – a mass spectrometric study of SOA aging, *Atmos. Chem. Phys.*, 12, 1483–1496, doi:10.5194/acp-12-1483-2012, 2012. 8590
- 5 Ng, N. L., Chhabra, P. S., Chan, A. W. H., Surratt, J. D., Kroll, J. H., Kwan, A. J., McCabe, D. C., Wennberg, P. O., Sorooshian, A., Murphy, S. M., Dalleska, N. F., Flagan, R. C., and Seinfeld, J. H.: Effect of NO_x level on secondary organic aerosol (SOA) formation from the photooxidation of terpenes, *Atmos. Chem. Phys.*, 7, 5159–5174, doi:10.5194/acp-7-5159-2007, 2007a. 8582, 8586
- 10 Ng, N. L., Kroll, J. H., Chan, A. W. H., Chhabra, P. S., Flagan, R. C., and Seinfeld, J. H.: Secondary organic aerosol formation from m-xylene, toluene, and benzene, *Atmos. Chem. Phys.*, 7, 3909–3922, doi:10.5194/acp-7-3909-2007, 2007b. 8582
- Ng, N. L., Canagaratna, M. R., Jimenez, J. L., Chhabra, P. S., Seinfeld, J. H., and Worsnop, D. R.: Changes in organic aerosol composition with aging inferred from aerosol mass spectra, *Atmos. Chem. Phys.*, 11, 6465–6474, doi:10.5194/acp-11-6465-2011, 2011. 8593
- 15 Noziere, B., Barnes, I., and Becker, K.-H.: Product study and mechanisms of the reactions of alpha-pinene and of pinonaldehyde with OH radicals, *J. Geophys. Res.-Atmos.*, 104, 23645–23656, 1999. 8582
- Offenberg, J. H., Lewandowski, M., Edney, E. O., Kleindienst, T. E., and Jaoui, M.: Influence of Aerosol Acidity on the Formation of Secondary Organic Aerosol from Biogenic Precursor Hydrocarbons, *Environ. Sci. Technol.*, 43, 7742–7747, doi:10.1021/es901538e, 2009. 8596
- 20 Paulot, F., Crouse, J. D., Kjaergaard, H. G., Kroll, J. H., Seinfeld, J. H., and Wennberg, P. O.: Isoprene photooxidation: new insights into the production of acids and organic nitrates, *Atmos. Chem. Phys.*, 9, 1479–1501, doi:10.5194/acp-9-1479-2009, 2009a. 8584, 8585
- 25 Paulot, F., Crouse, J. D., Kjaergaard, H. G., Kurten, A., St. Clair, J. M., Seinfeld, J. H., and Wennberg, P. O.: Unexpected epoxide formation in the gas-phase photooxidation of isoprene, *Science*, 325, 730–733, doi:10.1126/science.1172910, 2009b. 8584, 8585
- Presto, A. A., Hartz, K. E. H., and Donahue, N. M.: Secondary organic aerosol production from terpene ozonolysis. 2. Effect of NO_x concentration, *Environ. Sci. Technol.*, 39, 7046–7054, doi:10.1021/es050400s, 2005. 8582
- 30 Pye, H. O. T., Chan, A. W. H., Barkley, M. P., and Seinfeld, J. H.: Global modeling of organic aerosol: the importance of reactive nitrogen (NO_x and NO_3), *Atmos. Chem. Phys.*, 10, 11261–11276, doi:10.5194/acp-10-11261-2010, 2010. 8581

**α -pinene
photooxidation
particle phase
composition**

N. C. Eddingsaas et al.

Title Page

Abstract

Introduction

Conclusions

References

Tables

Figures

⏪

⏩

◀

▶

Back

Close

Full Screen / Esc

Printer-friendly Version

Interactive Discussion



- Shilling, J. E., Chen, Q., King, S. M., Rosenoern, T., Kroll, J. H., Worsnop, D. R., DeCarlo, P. F., Aiken, A. C., Sueper, D., Jimenez, J. L., and Martin, S. T.: Loading-dependent elemental composition of α -pinene SOA particles, *Atmos. Chem. Phys.*, 9, 771–782, doi:10.5194/acp-9-771-2009, 2009. 8582
- 5 Spittler, M., Barnes, I., Bejan, I., Brockmann, K. J., Benter, T., and Wirtz, K.: Reactions of NO_3 radicals with limonene and α -pinene: Product and SOA formation, *Atmos. Environ.*, 40, S116–S127, 2006. 8581
- St. Clair, J. M., McCabe, D. C., Crouse, J. D., Steiner, U., and Wennberg, P. O.: Chemical ionization tandem mass spectrometer for the in situ measurement of methyl hydrogen peroxide, *Rev. Sci. Instrum.*, 81, 094102, doi:10.1063/1.3480552, 2010. 8584
- 10 Surratt, J. D., Kroll, J. H., Kleindienst, T. E., Edney, E. O., Claeys, M., Sorooshian, A., Ng, N. L., Offenberg, J. H., Lewandowski, M., Jaoui, M., Flagan, R. C., and Seinfeld, J. H.: Evidence for Organosulfates in Secondary Organic Aerosol, *Environ. Sci. Technol.*, 41, 517–527, 2007. 8581
- 15 Surratt, J. D., Gomez-Gonzalez, Y., Chan, A. W. H., Vermeylen, R., Shahgholi, M., Kleindienst, T. E., Edney, E. O., Offenberg, J. H., Lewandowski, M., Jaoui, M., Maenhaut, W., Claeys, M., Flagan, R. C., and Seinfeld, J. H.: Organosulfate formation in biogenic secondary organic aerosol, *J. Phys. Chem. A*, 112, 8345–8378, doi:10.1021/jp802310p, 2008. 8581, 8585, 8591, 8592
- 20 Surratt, J. D., Chan, A. W. H., Eddingsaas, N. C., Chan, M. N., Loza, C. L., Kwan, A. J., Hersey, S. P., Flagan, R. C., Wennberg, P. O., and Seinfeld, J. H.: Reactive intermediates revealed in secondary organic aerosol formation from isoprene, *P. Natl. Acad. Sci.*, 107, 6640–6645, doi:10.1073/pnas.0911114107, 2010. 8588, 8594, 8595
- 25 Szmigielski, R., Surratt, J. D., Gomez-Gonzalez, Y., Van der Veken, P., Kourtchev, I., Vermeylen, R., Blockhuys, F., Jaoui, M., Kleindienst, T. E., Lewandowski, M., Offenberg, J. H., Edney, E. O., Seinfeld, J. H., Maenhaut, W., and Claeys, M.: 3-methyl-1,2,3-butanetricarboxylic acid: an atmospheric tracer for terpene secondary organic aerosol, *Geophys. Res. Lett.*, 34, L24811, doi:10.1029/2007GL031338, 2007. 8589, 8590
- 30 Taylor, W. D., Allston, T. D., Moscato, M. J., Fazekas, G. B., Kozlowski, R., and Takacs, G. A.: Atmospheric photo-dissociation lifetimes for nitromethane, methyl nitrite, and methyl nitrate, *Int. J. Chem. Kinet.*, 12, 231–240, 1980. 8583

**α -pinene
photooxidation
particle phase
composition**

N. C. Eddingsaas et al.

[Title Page](#)[Abstract](#)[Introduction](#)[Conclusions](#)[References](#)[Tables](#)[Figures](#)[Back](#)[Close](#)[Full Screen / Esc](#)[Printer-friendly Version](#)[Interactive Discussion](#)

- Warnke, J., Bandur, R., and Hoffmann, T.: Capillary-HPLC-ESI-MS/MS method for the determination of acidic products from the oxidation of monoterpenes in atmospheric aerosol samples, *Anal. Bioanal. Chem.*, 385, 34–45, doi:10.1007/s00216-006-0340-6, 2006. 8589
- 5 Yu, J., Cocker, David R., I., Griffin, R. J., Flagan, R. C., and Seinfeld, J. H.: Gas-phase ozone oxidation of monoterpenes: gaseous and particulate products, *J. Atmos. Chem.*, 34, 207–258, 1999a. 8582
- Yu, J., Griffin, R. J., Cocker, David R., I., Flagan, R. C., Seinfeld, J. H., and Blanchard, P.: Observation of gaseous and particulate products of monoterpene oxidation in forest atmospheres, *Geophys. Res. Lett.*, 26, 1145–1148, 1999b. 8581
- 10 Zhang, Y. Y., Müller, L., Winterhalter, R., Moortgat, G. K., Hoffmann, T., and Pöschl, U.: Seasonal cycle and temperature dependence of pinene oxidation products, dicarboxylic acids and nitrophenols in fine and coarse air particulate matter, *Atmos. Chem. Phys.*, 10, 7859–7873, doi:10.5194/acp-10-7859-2010, 2010. 8581, 8590

**α -pinene
photooxidation
particle phase
composition**

N. C. Eddingsaas et al.

Table 1. SOA yields from low- and high-NO_x photooxidation of α -pinene.

Sample ID	Oxidant	Seed	Temp. (°C)	HC (ppb)	Initial Vol. ($\mu\text{m}^3 \text{cm}^{-3}$)	ΔHC^a ($\mu\text{g m}^{-3}$)	$\Delta\text{M}_\text{O}^b$ ($\mu\text{g m}^{-3}$)	SOA Yield ^c (%)
1-H2O2	H ₂ O ₂	no seed	20–23	45.0±1.0	0.9±0.3	250±6	66.8±6.0	26.7±2.5
2-HONO	HONO	no seed	20–23	50.1±1.1	0.3±.2	260±6	20.0±2.3	7.7±0.9
3-H2O2	H ₂ O ₂	AS	20–25	48.5±1.1	11.0±0.4	265±6	76.6±6.7	28.9±2.6
4-HONO	HONO	AS	20–23	52.4±1.2	12.0±0.7	258±7	37.2±3.0	14.4±1.1
5-H2O2	H ₂ O ₂	AS + SA	20–25	46.9±1.1	9.3±0.58	264±6	72.9±7.0	27.6±2.8
6-HONO	HONO	AS + SA	20–23	45.5±1.0	16.0±1.1	225±6	39.6±4.5	17.6±1.9
7-H2O2	H ₂ O ₂	no seed	20–25	19.8±0.5	0.5±0.2	109±3	40.0±3.1	36.7±3.0
8-MeONO	CH ₃ ONO	no seed	20–23	38.9±1.0	5.1±0.2	208±6	51.9±3.8	25.4±1.7
9-H2O2	H ₂ O ₂	AS	20–25	46.8±1.1	9.4±0.4	254±6	71.6±6.2	28.2±2.5
10-MeONO	CH ₃ ONO	AS	20–23	47.9±1.1	10.5±0.5	249±6	60.3±4.9	24.2±1.9
11-H2O2	H ₂ O ₂	AS + SA	20–25	46.8±1.1	8.5±0.4	256±6	70.4±6.2	27.5±2.5
12-MeONO	CH ₃ ONO	AS + SA	20–23	43.7	14	242	42.6	17.6
13-H2O2	H ₂ O ₂	AS	20–25	45.0±1.0	13.7±0.6	247±6	63.5±5.6	25.7±2.3
14-MeONO	CH ₃ ONO	AS	20–23	44.9±1	15.4±0.6	250±6	54.0±4.3	21.6±1.8

^a ΔHC : mass concentration of α -pinene reacted.^b ΔM_O : mass concentration of SOA.^c SOA yield is maximum mass concentration of SOA formed divided by the mass concentration of α -pinene reacted.

Title Page

Abstract

Introduction

Conclusions

References

Tables

Figures

⏪

⏩

◀

▶

Back

Close

Full Screen / Esc

Printer-friendly Version

Interactive Discussion



**α -pinene
photooxidation
particle phase
composition**

N. C. Eddingsaas et al.

Table 2. Raw peak areas from UPLC chromatograms of carboxylic acids, organosulfates, and nitroxy organosulfates from the photooxidation of α -pinene.

SOA component ([M – H] [−])	H ₂ O ₂		HONO		MeONO	
	AS	AS + SA	AS	AS + SA	AS	AS + SA
2-Hydroxyterpenylic acid (187)	–	–	1918	824	2285	1509
Terpenylic acid (171)	2097	2522	911	933	1152	1255
3-methyl-1,2,3-butanetricarboxylic acid (3-MBTCA) (203)	458	702	307	337	910	1231
Diaterpenylic acid acetate (231)	318	763	1984	401	1658	1728
10-Hydroxypinonic acid (199)	2229	1760	361	426	314	662
Pinic acid (185)	1552	1469	–	–	–	–
Pinonic acid (183)	1155	1297	–	–	–	–
Sulfate of 10-hydroxy pinonic acid (279)	–	723	–	1185	–	1343
α -pinene hydroxy sulfate (249)	–	1692	–	1904	–	933
Ring opened carbonyl nitrate sulfate (310)	–	–	–	1744	–	1075
<i>m/z</i> 247.07 (C ₁₀ H ₁₅ O ₅ S)	–	–	–	3193	–	435
<i>m/z</i> 265.07 (C ₁₀ H ₁₇ O ₆ S)	–	–	–	219	–	229
<i>m/z</i> 294.06 (C ₁₀ H ₁₆ NO ₇ S)	–	–	–	1799	–	–
<i>m/z</i> 295.05 (C ₁₀ H ₁₅ O ₈ S)	–	–	–	494	–	–
<i>m/z</i> 296.04 (C ₁₀ H ₁₄ NO ₈ S)	–	–	–	108	–	–
<i>m/z</i> 328.07 (C ₁₀ H ₁₈ NO ₉ S)	–	–	–	345	–	–
<i>m/z</i> 342.05 (C ₁₀ H ₁₆ NO ₁₀ S)	–	–	–	110	–	–

Title Page

Abstract

Introduction

Conclusions

References

Tables

Figures

⏪

⏩

◀

▶

Back

Close

Full Screen / Esc

Printer-friendly Version

Interactive Discussion



α -pinene photooxidation particle phase composition

N. C. Eddingsaas et al.

Table 3. Peak areas scaled to low-NO_x AS seed SOA loading from UPLC chromatograms of carboxylic acids, organosulfates, and nitrooxy organosulfates from the photooxidation of α -pinene.

SOA component ([M – H] [−])	H ₂ O ₂		HONO		MeONO	
	AS	AS + SA	AS	AS + SA	AS	AS + SA
2-Hydroxyterpenylic acid (187)	–	–	4480	1426	3167	2617
Terpenylic acid (171)	2097	2451	2128	1615	1597	2177
3-methyl-1,2,3-butanetricarboxylic acid (3-MBTCA) (203)	458	682	717	583	1261	2135
Diaterpenylic acid acetate (231)	318	742	4635	695	2298	2997
10-Hydroxypinonic acid (199)	2229	1711	843	737	435	1148
Pinic acid (185)	1552	1428	–	–	–	–
Pinonic acid (183)	1155	1261	–	–	–	–
Sulfate of 10-hydroxy pinonic acid (279)	–	703	–	2051	–	2329
α -pinene hydroxy sulfate (249)	–	1645	–	3296	–	1618
Ring opened carbonyl nitrate sulfate (310)	–	–	–	3019	–	1865
<i>m/z</i> 247.07 (C ₁₀ H ₁₅ O ₅ S)	–	–	–	5527	–	755
<i>m/z</i> 265.07 (C ₁₀ H ₁₇ O ₆ S)	–	–	–	379	–	397
<i>m/z</i> 294.06 (C ₁₀ H ₁₆ NO ₇ S)	–	–	–	3114	–	–
<i>m/z</i> 295.05 (C ₁₀ H ₁₅ O ₈ S)	–	–	–	855	–	–
<i>m/z</i> 296.04 (C ₁₀ H ₁₄ NO ₈ S)	–	–	–	187	–	–
<i>m/z</i> 328.07 (C ₁₀ H ₁₈ NO ₉ S)	–	–	–	597	–	–
<i>m/z</i> 342.05 (C ₁₀ H ₁₆ NO ₁₀ S)	–	–	–	190	–	–

Title Page

Abstract

Introduction

Conclusions

References

Tables

Figures

⏪

⏩

◀

▶

Back

Close

Full Screen / Esc

Printer-friendly Version

Interactive Discussion

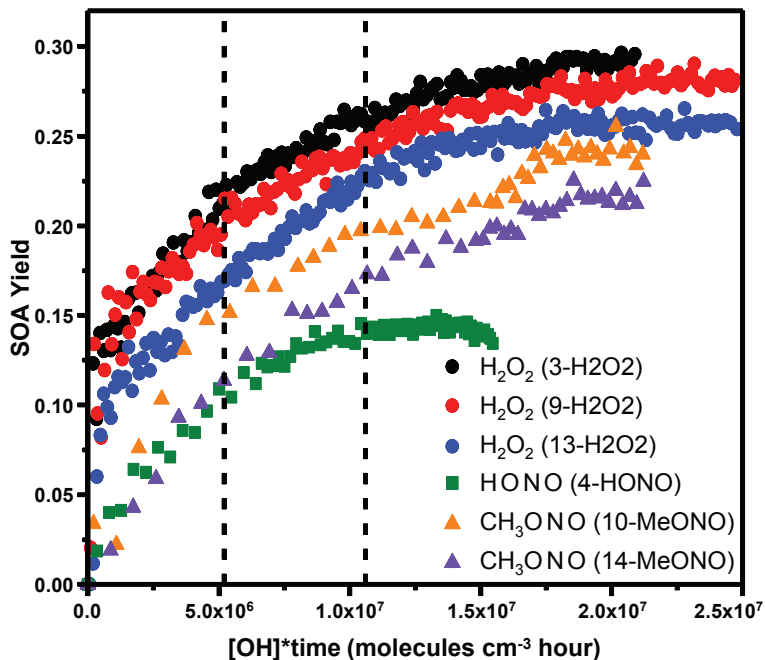


Fig. 1. SOA yield as a function of OH exposure of α -pinene from low- NO_x , high-NO, and high- NO_2 OH oxidation in the presence of ammonium sulfate seed particles. The vertical dashed lines represent one and two α -pinene lifetimes with respect to reaction with OH. The OH source and sample ID for each experiment is shown in the figure.

**α -pinene
photooxidation
particle phase
composition**

N. C. Eddingsaas et al.

Title Page	
Abstract	Introduction
Conclusions	References
Tables	Figures
⏪	⏩
◀	▶
Back	Close
Full Screen / Esc	
Printer-friendly Version	
Interactive Discussion	



α -pinene photooxidation particle phase composition

N. C. Eddingsaas et al.

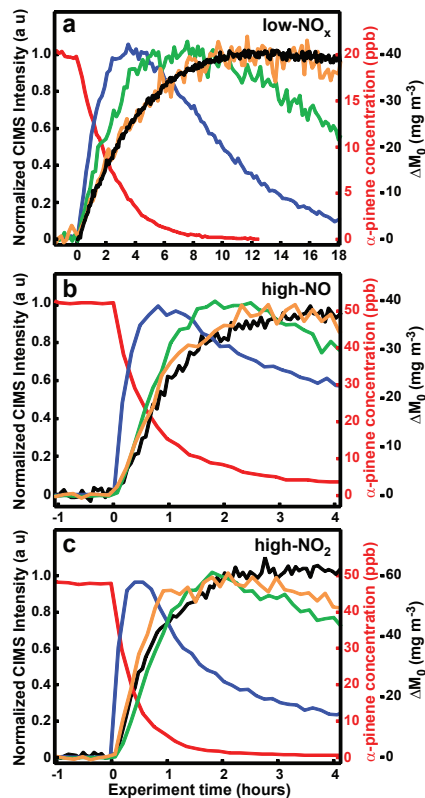


Fig. 2. Time evolution of SOA growth along with gas-phase time profile of first- and second-generation products of OH oxidation of α -pinene under (a) low- NO_x conditions (7-H₂O₂), (b) high-NO conditions (4-HONO), and (c) high- NO_2 conditions (10-MeONO). In all plots, the red line is α -pinene, blue line is pinonaldehyde, and black line is SOA growth. In (a) green is 10-hydroxy pinonic/pinonic peracid and orange is pinonic acid, (b, c) green is pinonaldehyde PAN, and orange is pinonaldehyde nitrate.

**α -pinene
photooxidation
particle phase
composition**

N. C. Eddingsaas et al.

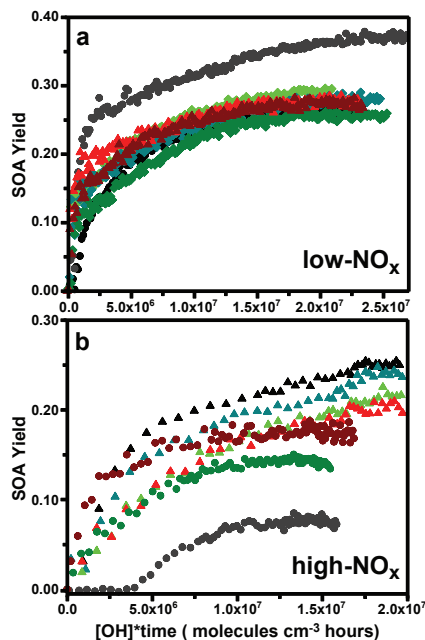


Fig. 3. SOA yield as a function of OH exposure of α -pinene OH oxidation in the presence of no (black, grey), neutral (shades of green), or acidic (shades of red) seed particles under **(a)** low-NO_x conditions and **(b)** high-NO_x conditions where photolysis of HONO (dots) or methyl nitrite (triangles) is the OH source. The sample IDs for each experiment are **(a)** black dots (1-H₂O₂), grey dots (7-H₂O₂), light green diamonds (3-H₂O₂), teal diamonds (9-H₂O₂), green diamonds (13-H₂O₂), red triangles (5-H₂O₂), dark red triangles (11-H₂O₂) **(b)** grey dots (2-HONO), black triangles (8-MeONO), green dots (4-HONO), light green triangles (10-MeONO), teal triangles (14-MeONO), dark red dots (6-HONO), and red triangles (12-MeONO). The low-NO_x experiment that resulted in greater SOA yield (grey points in panel a (7-H₂O₂)) is from 20 ppb of α -pinene, all other data is from the OH oxidation of ~50 ppb of α -pinene.

Title Page

Abstract

Introduction

Conclusions

References

Tables

Figures

◀

▶

◀

▶

Back

Close

Full Screen / Esc

Printer-friendly Version

Interactive Discussion

**α -pinene
photooxidation
particle phase
composition**

N. C. Eddingsaas et al.

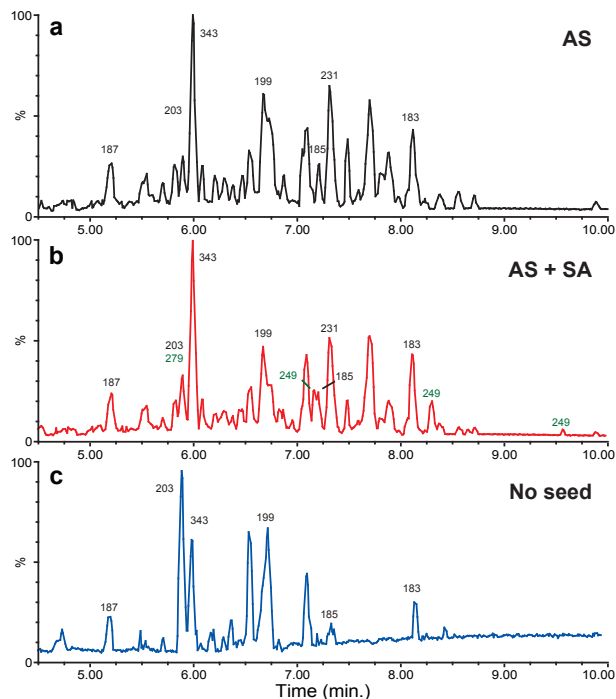


Fig. 4. UPLC/(-)ESI-TOF chromatograms from the filter samples of low- NO_x photooxidation of α -pinene or pinonaldehyde, **(a)** α -pinene in the presence of AS seed particles (3- H_2O_2) **(b)** α -pinene in the presence of AS + SA seed particles (5- H_2O_2) and **(c)** pinonaldehyde. Chromatographic peaks designated with black $[\text{M} - \text{H}]^-$ ions are carboxylic acids and chromatographic peaks designated with green $[\text{M} - \text{H}]^-$ ions are organosulfates. See Table 2 for compound names.

Title Page

Abstract

Introduction

Conclusions

References

Tables

Figures

◀

▶

◀

▶

Back

Close

Full Screen / Esc

Printer-friendly Version

Interactive Discussion

**α -pinene
photooxidation
particle phase
composition**

N. C. Eddingsaas et al.

Title Page

Abstract

Introduction

Conclusions

References

Tables

Figures

◀

▶

◀

▶

Back

Close

Full Screen / Esc

Printer-friendly Version

Interactive Discussion

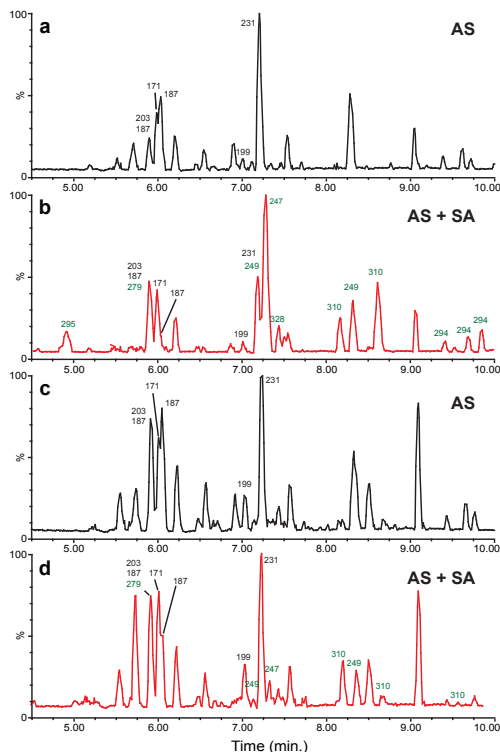


Fig. 5. UPLC/(-)ESI-TOF chromatograms from the filter samples of high-NO_x photooxidation of α -pinene. **(a)** HONO was the OH source, AS seed particles (4-HONO) **(b)** HONO was the OH source, AS + SA seed particles (6-HONO), **(c)** CH₃ONO was the OH source, AS seed particles (10-MeONO), and **(d)** CH₃ONO was the OH source, AS + SA seed particles (12-MeONO). Chromatographic peaks designated with black [M – H][–] ions are carboxylic acids and chromatographic peaks designated with green [M – H][–] ions are organosulfates and nitroxy organosulfates. See Table 2 for compound names.

**α -pinene
photooxidation
particle phase
composition**

N. C. Eddingsaas et al.

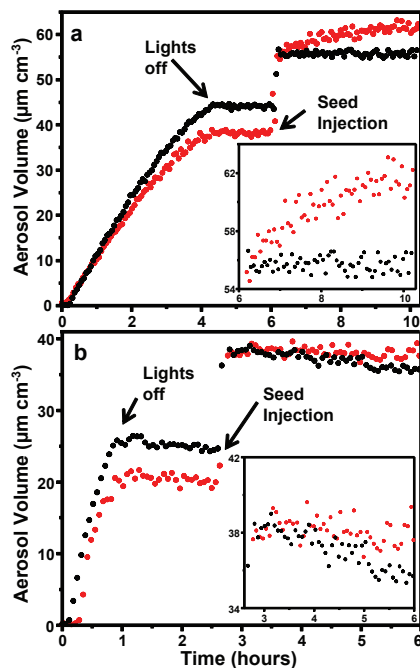


Fig. 6. Time traces of aerosol volume as a result of SOA growth from OH oxidation of α -pinene followed by injection of ammonium sulfate seed (black) or ammonium sulfate and sulfuric acid seed (red) under **(a)** low- NO_x and **(b)** high- NO_x (methyl nitrite photolysis) conditions. The difference in the quantity of self-nucleated aerosol volume growth from both **(a)** low- and **(b)** high- NO_x experiments is due to greater gas-phase α -pinene concentration at the beginning of each of the AS seed experiments compared to the AS + SA experiments.

Title Page

Abstract

Introduction

Conclusions

References

Tables

Figures

◀

▶

◀

▶

Back

Close

Full Screen / Esc

Printer-friendly Version

Interactive Discussion

α -pinene photooxidation particle phase composition

N. C. Eddingsaas et al.

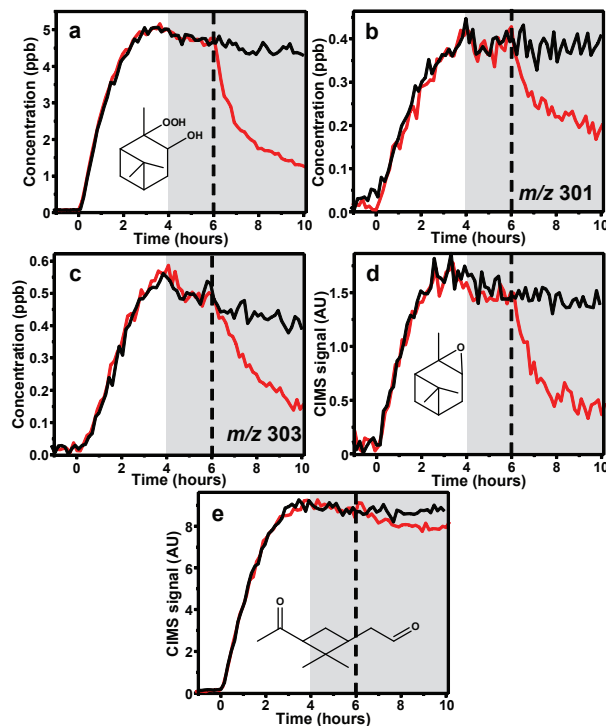


Fig. 7. CIMS traces of α -pinene OH oxidation under low- NO_x conditions, photooxidation for four hours, lights off and contents in the dark for two hours followed by injection of ammonium sulfate seed (black) or ammonium sulfate and sulfuric acid seed (red). Shaded grey area is when the chamber was dark and the dashed line indicates when aerosol seed was added.

[Title Page](#)
[Abstract](#)
[Introduction](#)
[Conclusions](#)
[References](#)
[Tables](#)
[Figures](#)
[◀](#)
[▶](#)
[◀](#)
[▶](#)
[Back](#)
[Close](#)
[Full Screen / Esc](#)
[Printer-friendly Version](#)
[Interactive Discussion](#)

**α -pinene
photooxidation
particle phase
composition**

N. C. Eddingsaas et al.

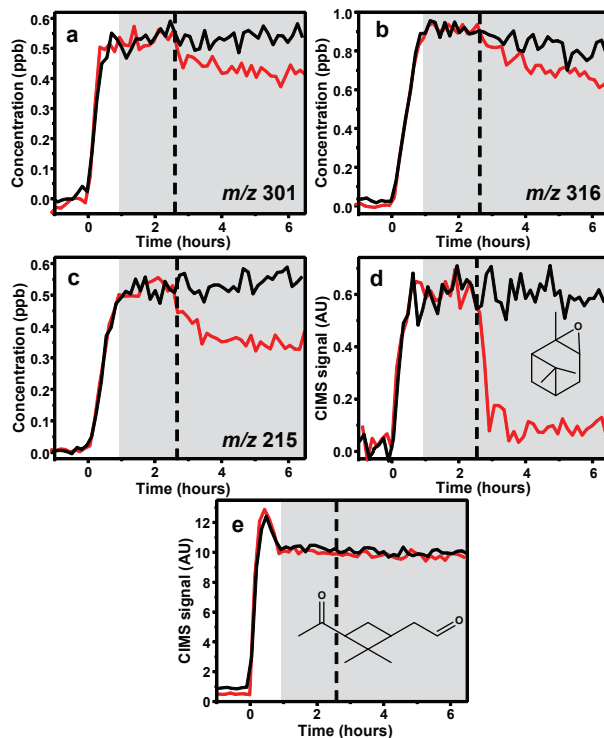


Fig. 8. CIMS traces of α -pinene OH oxidation under high- NO_x conditions, photooxidation for ~ 0.8 h, lights off and contents in the dark for ~ 2 h followed by injection of ammonium sulfate seed (black) or ammonium sulfate and sulfuric acid seed (red). Shaded grey area is when the chamber was dark and the dashed line indicates when aerosol seed was added.

Title Page

Abstract

Introduction

Conclusions

References

Tables

Figures

◀

▶

◀

▶

Back

Close

Full Screen / Esc

Printer-friendly Version

Interactive Discussion